*Desalination and Water Treatment*
www.deswater.com
51 (2013) 1641–1650
February
1944-3994/1944-3986 © 2013 Desalination Publications. All rights reserved
doi: 10.1080/19443994.2012.695048
Taylor & Francis
Taylor & Francis Group

# Turbidity and pH dissipations in a dosage of high concentration NaOH solution to seawater

V. Kesler[a], D. Hasson[a,*], H. Shemer[a], R. Semiat[a], C. Bartels[b], M. Wilf[c]

[a]*Rabin Desalination Laboratory, Technion-Israel Institute of Technology, Haifa, Israel*
*Tel. +972 48292936; Fax: +972 8295672; email: hasson@tx.technion.ac.il*
[b]*Hydranautics, Research and Development, Oceanside, CA, USA*
[c]*Consultant RO Technology, San Diego, CA, USA*

Received 5 March 2012; Accepted 10 May 2012

ABSTRACT

It is sometimes necessary to dose into a desalination feed stream a caustic solution to achieve a controlled pH increase, as, for example, in the application of boron suppression measures. To restrict the size of the caustic feed system, the NaOH is dosed from a high concentration solution. The solution is injected at the center of the raw water feed pipe and its concentration dissipates as it mixes with the main flowing solution. The problem is that desalination feed waters usually contain ions of a sparingly soluble salt such as $CaCO_3$ and $Mg(OH)_2$, which tend to precipitate at high pH levels. The very high local concentrations of the dosed NaOH at the injection region can lead to very high local supersaturations and induce the nucleation and precipitation of scale particles. The main goal of the present work was to delineate flow and concentration conditions at which dosage of a concentrated NaOH solution to seawater concentrates will not induce significant precipitation of $CaCO_3$ and $Mg(OH)_2$.

*Keywords:* Seawater; NaOH dosage; Desalination; Scale precipitation; Dissipation model

## 1. Introduction

Mixing is a widely used operation in the process industries and its purpose is to produce a uniform phase. It can be achieved using mechanical mixers, fluid jet mixers, static mixers, or pipeline with tees. In the present work, we consider mixing achieved by injecting a solution through a capillary jet located at the center of a tube through which there is flow of the main solution.

The present study was motivated by the problem of controlling boron concentration in RO seawater desalination by a pH increase through NaOH dosage. To restrict the size of the caustic feed system, the NaOH is dosed from a high concentration solution. The solution is injected at the center of the raw water feed pipe and its concentration dissipates as it mixes with the main flowing solution.

The problem is that desalination feed solutions usually contain ions of sparingly soluble salts such as $CaCO_3$ and $Mg(OH)_2$, which tend to precipitate at high pH levels. The high local concentration of the NaOH at the injection region can lead to very high local supersaturations and induce nucleation and precipitation of the scale particles. Such parti-

*Corresponding author.

*Presented at the International Conference on Desalination for the Environment, Clean Water and Energy, European Desalination Society, 23–26 April 2012, Barcelona, Spain*

cles will settle on the membrane and can lead to a significant decrease in permeate production capacity.

The effects of geometry and Reynolds number on the turbulent mixing of reactants were studied by Singh and Toor [1]. They developed a generalized correlation for the mixing induced by injecting a jet into stream flowing in a pipe. It was assumed that in the inlet region the mixing depends upon the jet turbulence and in the far downstream region the mixing depends upon the pipe turbulence. Experimental data of several studies were successfully correlated by the following two equations:

$$d^2 = 60\,\mathrm{Re}_j^{-0.4} \cdot \exp\left(-3.2\frac{Z^{0.5}}{\mathrm{Re}_j^{0.15}}\right) \quad (1)$$

while the fully developed region data fitted the equation:

$$d^2 = 0.062 \cdot \frac{\mathrm{Re}_j^{0.525}}{Z^{1.75}} \quad (2)$$

The non-dimensional average concentration $d^2$ is given by:

$$d^2 = \frac{\bar{c}^2}{\bar{c}_0^2} \quad (3)$$

where $\bar{c}$ is the average concentration at the axial distance $z$ and $\bar{c_0}$ is the concentration at the jet entrance.

The non-dimensional axial distance $Z$ is given by:

$$Z = \frac{z}{d_j} \quad (4)$$

The Reynolds number $\mathrm{Re}_j = \frac{\rho V d_j}{\mu}$ is based on the jet velocity $V$, the jet diameter $d_j$, the injected solution density $\rho$, and the injection solution viscosity $\mu$.

The main goal of the present work was to delineate the flow and concentration conditions at which dosage of a concentrated NaOH solution to seawater concentrates does not induce significant precipitation of $CaCO_3$ and $Mg(OH)_2$.

## 2. Experimental

### 2.1. Experimental system

The experimental system is sketched in Fig. 1. A simulated Pacific Ocean seawater solution (Table 1) was fed to the top of a glass tube (50 mm diameter,

Table 1
Simulated Pacific Seawater solution

| Component | Concentration (ppm) |
|---|---|
| $Ca^{2+}$ | 356 |
| $K^+$ | 362 |
| $Mg^{2+}$ | 1,200 |
| $Na^+$ | 10,670 |
| $HCO_3^-$ | 133 |
| $SO_4^{2-}$ | 2,500 |
| $Cl^-$ | 18,700 |
| pH = 8 | TDS = 34,000 |

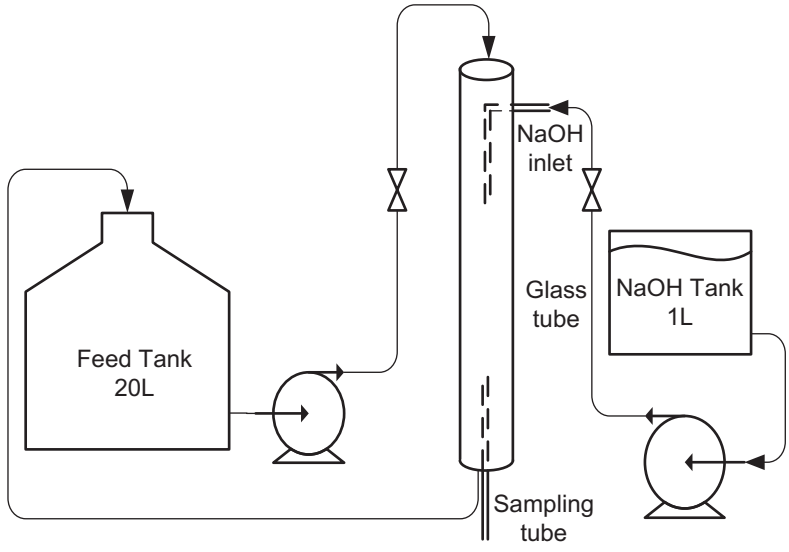


Fig. 1. Schematic diagram of the experimental system.

1,000 mm long) and recycled to the feed tank. A concentrated NaOH solution of 10 mol/L was injected through a capillary tube of 2 mm diameter located at the center of the glass tube. The pH of the feed tank was maintained constant at the level of 8 by the pH controlled addition of HCl solution. A movable tube located at the bottom of the pipe was used to sample the flowing seawater along the tube axis.

### 2.2. Experimental program

The experiments were carried out at seawater flow rates in the range of 9.5–22.8 L/min providing flow velocities of 8.1–19.4 cm/s. The NaOH solution was injected at a flow rate in the range of 0.48–2.85 ml/min providing flow velocities in the range of 0.25–1.5 cm/s.

The runs were carried out at three seawater flow rates corresponding to Reynolds numbers of 4,000, 8,000, and 9,600, respectively. The flow rate of the NaOH solution was controlled such that a dosage of 20, 30, 40, or 50 ppm was injected into the seawater.

Each run was repeated three times. Reproducibility of the data was satisfactory so that averaged values are here presented. Experimental conditions are summarized in Table 2. All the runs were carried out at room temperature (25–27˚C).

### 2.3. Measurement technique

The high supersaturation level of the samples can lead to significant changes in solution composition in the period extending from the sampling instant to the measurement time. Figs. 2 and 3 illustrate the changes in turbidity and in pH, respectively, that occurred at the axial distance of 1 cm in the run performed at a Reynolds number of 8,000 and a NaOH dosage of 50 ppm. Data free from the sampling time error were determined by extrapolating the experimental measurements to zero time. For the data of Fig. 2, the zero time extrapolated turbidity was 222 NTU and for the data of Fig. 3 the extrapolated pH was 10.81.

Table 3 lists the turbidity change values in two minutes and the zero time turbidity estimate based on two repeat measurements in samples taken at various axial distances. Similar data for the pH are given in Table 4.

## 3. Results

### 3.1. Turbidity dissipation at various NaOH dosages and seawater flows.

Figs. 4 and 5 illustrate the typical turbidity profiles along the axial distance for the runs carried out with a NaOH dosage of 30 ppm at seawater flow Reynolds numbers of 8,000 and 9,600, respectively. The turbidity level is seen to initially decrease at a very rapid rate within a short axial distance of a few centimeters and subsequently to converge rapidly to an asymptotic limit at which the turbidity level is negligible (1–3 NTU).

Table 5 summarizes the effects of NaOH dosage and of the seawater flow rate on turbidity dissipation. The NaOH dosage has a significant effect on the extent of axial dissipation distance. For instance, at Re = 8,000, increase of the NaOH dosage from 20 to 50 ppm augments the dissipation distance from 4.5 to 15 cm. Increase of the Reynolds number has a moder-

Table 2
Experimental conditions investigated

| Seawater Reynolds No. | NaOH dosage (ppm) | NaOH flow (ml/min) | NaOH velocity (cm/s) | NaOH solution Reynolds No. | Seawater flow (L/min) | Seawater velocity (cm/s) |
|---|---|---|---|---|---|---|
| 4,000 | 20 | 0.48 | 0.25 | 0.66 | 9.5 | 8.1 |
| 4,000 | 30 | 0.74 | 0.39 | 0.99 | 9.5 | 8.1 |
| 4,000 | 40 | 0.95 | 0.5 | 1.32 | 9.5 | 8.1 |
| 4,000 | 50 | 1.19 | 0.63 | 1.65 | 9.5 | 8.1 |
| 8,000 | 20 | 0.95 | 0.5 | 1.32 | 19 | 16.1 |
| 8,000 | 30 | 1.48 | 0.79 | 1.98 | 19 | 16.1 |
| 8,000 | 40 | 1.9 | 1 | 2.64 | 19 | 16.1 |
| 8,000 | 50 | 2.38 | 1.25 | 3.28 | 19 | 16.1 |
| 9,600 | 20 | 1.14 | 0.6 | 1.58 | 22.8 | 19.4 |
| 9,600 | 30 | 1.78 | 0.94 | 2.38 | 22.8 | 19.4 |
| 9,600 | 40 | 2.28 | 1.21 | 3.17 | 22.8 | 19.4 |
| 9,600 | 50 | 2.85 | 1.5 | 3.94 | 22.8 | 19.4 |

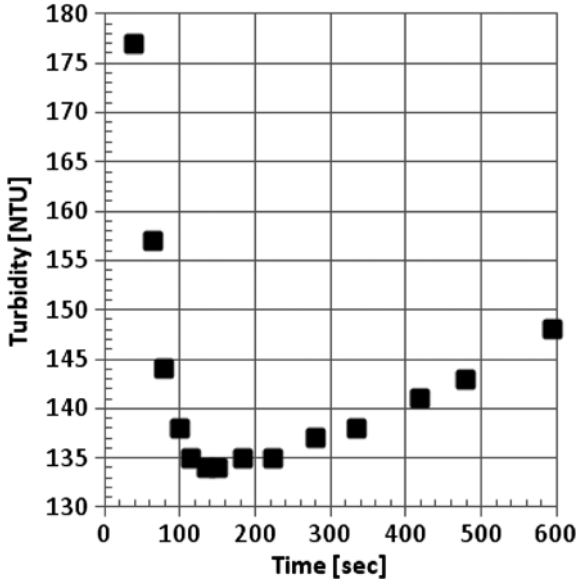


Fig. 2. Turbidity changes in the sample taken at $z = 1$ cm (Re = 8,000, 50 ppm NaOH).

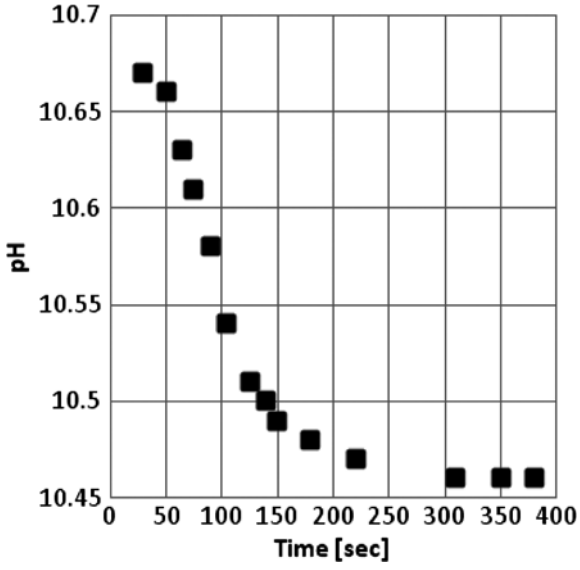


Fig. 3. pH changes in the sample taken at $z = 1$ cm (Re = 8,000, 50 ppm NaOH).

ate effect. At a dosage of 50 ppm, increase of the Reynolds number from 4,000 to 9,600 augments the dissipation distance from 10 to 15 cm.

### 3.2. pH decay at various NaOH dosages and seawater flows

Figs. 6 and 7 illustrate the typical OH concentration profiles along the axial distance for runs carried out at a seawater flow Reynolds number of 8,000 with a NaOH dosage of 30 and 40 ppm, respectively. Whereas the turbidity decline along the axial distance

Table 3
Zero time extrapolation of turbidity measurements

| Sample location $z$ (cm) | Run | Turb. changes in 120 s (NTU) | Zero time turb. (NTU) |
|---|---|---|---|
| 0.1 | A | 226–189 | 256 |
| | B | 235–202 | 242 |
| 2 | C | 65–50 | 75.5 |
| | D | 66–51 | 74.7 |
| 4 | E | 21.9–19.4 | 25.7 |
| | F | 23.5–20.4 | 24.5 |

Table 4
Zero time extrapolation of pH measurements

| Sample location $z$ (cm) | Run | pH changes in 120 s | Zero time pH |
|---|---|---|---|
| 0.1 | A | 13.2–13.3 | 13.23 |
| | B | 13.24–13.44 | 13.17 |
| 1 | C | 10.67–10.46 | 10.75 |
| | D | 10.7–10.52 | 10.78 |
| 1.5 | E | 10.57–10.53 | 10.65 |
| | F | 10.60–10.58 | 10.65 |

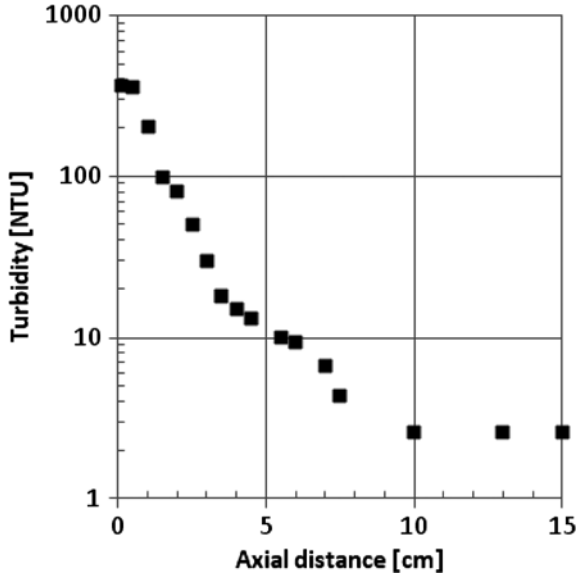


Fig. 4. Turbidity as a function of axial distance (Re = 8,000, 30 ppm NaOH).

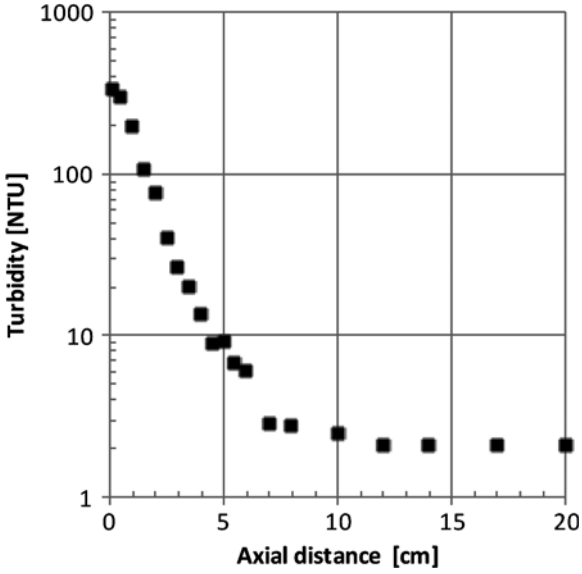


Fig. 5. Turbidity as a function of axial distance (Re = 9,600, 30 ppm NaOH).

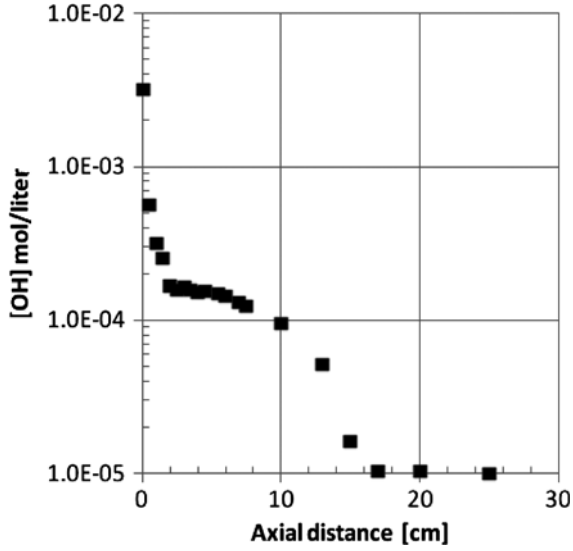


Fig. 6. OH concentration as a function of axial distance (Re = 8,000, 30 ppm NaOH).

was continuous, the OH concentration decay in most cases showed four distinct zones: an initial zone in which there was an abrupt sharp drop in the OH level, an intermediate zone in which the OH level declined very slightly over a substantial distance, a third zone in which the OH level declined continuously, and a fourth zone in which the OH level reached a terminal asymptotic value. Table 6 summarizes the data on the extent of the intermediate zone and the final pH level.

### 3.3. Decay of calcite SI at various NaOH dosages and seawater flows

The driving forces causing precipitation are the supersaturation levels of the flowing solution with respect to $CaCO_3$ and $Mg(OH)_2$. The supersaturation of $CaCO_3$ is expressed by the Saturation Index (SI) given by the activity product of the ions divided by the solubility constant:

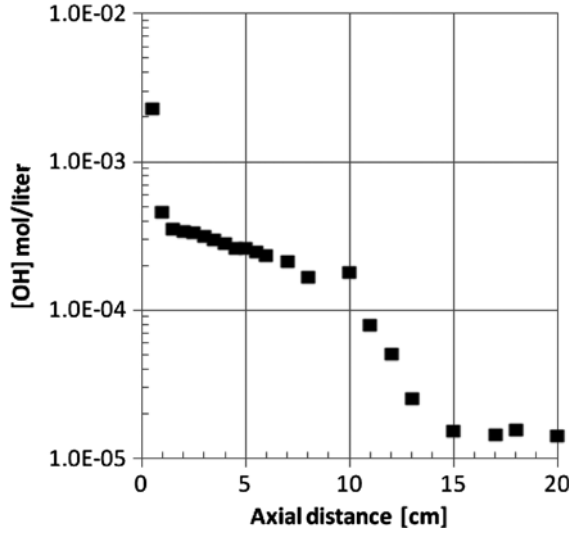


Fig. 7. OH concentration as a function of axial distance (Re = 8,000, 40 ppm NaOH).

Table 5
Effects of NaOH dosage and seawater Reynolds number on the turbidity dissipation

| NaOH dosage (ppm) | Re = 4,000 | | Re = 8,000 | | Re = 9,600 | |
|---|---|---|---|---|---|---|
| | Distance at final turbidity (cm) | Time for final turbidity (ms) | Distance at final turbidity (cm) | Time for final turbidity (ms) | Distance at final turbidity (cm) | Time for final turbidity (ms) |
| 20 | 4 | 50 | 4.5 | 28 | 5 | 26 |
| 30 | 7 | 87 | 10 | 62 | 12 | 62 |
| 40 | 8 | 99 | 12 | 74 | 12 | 62 |
| 50 | 10 | 116 | 15 | 93 | 15 | 78 |

Table 6
Effects of NaOH dosage and Reynolds number on the pH dissipation

| Re = 4,000 | | | | | Re = 8,000 | | | | Re = 9,600 | | | | |
|---|---|---|---|---|---|---|---|---|---|---|---|---|---|
| NaOH dosage (ppm) | Initial pH level | Interm. pH level | Length interm. zone (cm) | Final pH level | NaOH dosage (ppm) | Initial pH level | Interm. pH level | Length interm. zone (cm) | Final pH level | NaOH dosage (ppm) | Initial pH level | Interm. pH level | Length interm. zone (cm) | Final pH level |
| 20 | 10.8 | 9.2–9.5 | 2 | 8.7 | 20 | 11.4 | 10.1–10.3 | 3 | 8.7 | 20 | 11.6 | 10.1–10.3 | 4 | 8.7 |
| 30 | 10.6 | 10.1–10.2 | 5 | 8.9 | 30 | 11.5 | 10.1–10.2 | 5.5 | 9 | 30 | 12.4 | 10.2–10.4 | 5.5 | 9.05 |
| 40 | 11.7 | 10.25–10.4 | 5 | 9.2 | 40 | 12.5 | 10.25–10.5 | 8.5 | 9.2 | 40 | 12.2 | 10.3–10.5 | 8 | 9.2 |
| 50 | 11.6 | 10.3–10.5 | 8 | 9.7 | 50 | 13.5 | 10.3–10.6 | 15 | 9.7 | 50 | 13.1 | 10.3–10.6 | 11 | 9.6 |

$$SI = \frac{(a_{Ca^{2+}})(a_{CO_3^{2-}})}{K_{sp(calcite)}} \quad (5)$$

Values of the SI were evaluated using the GWB software [2].

Figs. 8 and 9 illustrate the typical axial profiles of calcite SI for the runs carried out at Re = 8,000 with NaOH dosages of 30 and 40 ppm, respectively.

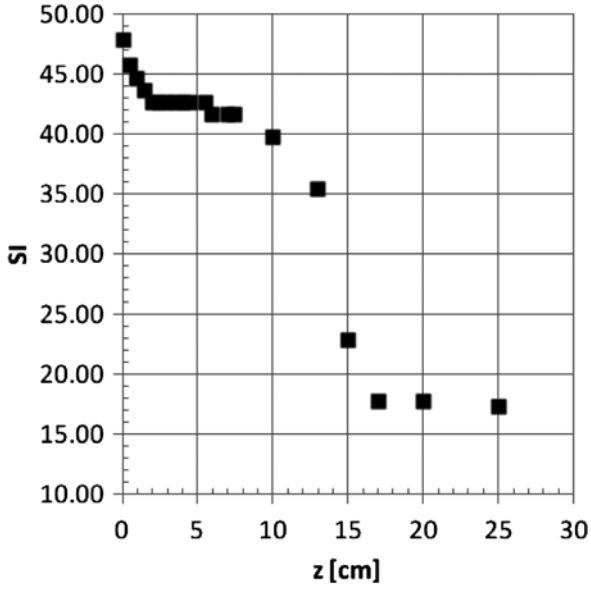


Fig. 8. SI of calcite as a function of axial distance (Re = 8,000, 30 ppm NaOH).

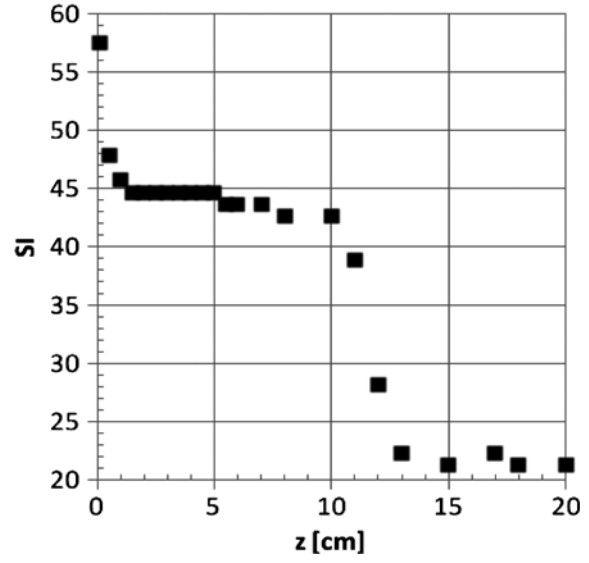


Fig. 9. SI of calcite as a function of axial distance (Re = 8,000, 40 ppm NaOH).

The decay in the SI of calcite displayed similar characteristics to the pH decay behavior. The SI changes, exemplified by the data in Fig. 9, were as follows:

- An initial zone displaying a sharp drop in the SI level (SI = 55–44.7 at $z$ = 0–1 cm).
- An intermediate zone displaying a very slight SI of decline over a substantial distance (SI = 44.7–42.7 at $z$ = 1–8 cm).
- A third zone displaying a continuous SI decline.
- A fourth zone in which the SI level reaches a terminal asymptotic value (SI = 22.4).

Table 7 summarizes the data on the extent of intermediate zone and the final SI level of calcite. The existence of a constant SI in the intermediate zone is possibly due to two opposing effects. As the jet flows down, the $CaCO_3$ precipitation reduces the Ca and carbonate concentrations. This generates a diffusive effect causing the Ca and carbonate ions to move toward the tube center. These two counteracting effects can lead to a constant level of the SI in the intermediate zone.

Some support to this hypothesis is provided by visual evidence. Figs. 10 and 11 show the photographs of the jet flow in the runs carried out at Reynolds number 8,000 at 30 and 40 ppm NaOH dosages, respectively. The extent of the intermediate zone roughly coincides with the distance at which the jet reaches the tube's walls. Since the diffusive effect supplying Ca and carbonate ions is arrested once the jet spreads to the walls of the tube, the SI can start to decrease only beyond this point.

### 3.4. Decay of SI of brucite at various NaOH dosages and seawater flows

The SI of brucite is defined by:

$$\mathrm{SI} = \frac{(a_{\mathrm{Mg}^{2+}})(a_{\mathrm{OH}^-})^2}{K_{\mathrm{sp(Brucite)}}} \quad (6)$$

Figs. 12 and 13 illustrate the typical profiles of the SI of brucite along the axial distance for the runs carried out at a seawater flow Reynolds number of 8,000 with NaOH dosages of 30 and 40 ppm, respectively. The decay of the SI of brucite also showed four distinct zones: an initial zone in which there was an abrupt sharp drop in the SI of brucite, an intermediate zone in which the SI of brucite declined very slightly over a substantial distance, a third zone in which the SI of

Table 7
Effects of NaOH dosage and Reynolds number on calcite SI dissipation

| Re = 4,000 | | | | | Re = 8,000 | | | | | Re = 9,600 | | | | |
|---|---|---|---|---|---|---|---|---|---|---|---|---|---|---|
| NaOH dosage (ppm) | Initial SI level | Interm. SI level | Length interm. zone (cm) | Final SI level | NaOH dosage (ppm) | Initial SI level | Interm. SI level | Length interm. zone (cm) | Final SI level | NaOH dosage (ppm) | Initial SI level | Interm. SI level | Length interm. zone (cm) | Final SI level |
| 20 | 46.2 | – | – | 10.5 | 20 | 47.9 | 43.7–41.7 | 3 | 10.7 | 20 | 49.90 | 43.65–40.7 | 4 | 10.7 |
| 30 | 45.7 | 41.7–40.7 | 2.5 | 15.1 | 30 | 47.9 | 42.7–41.7 | 5.5 | 17.4 | 30 | 56.2 | 43.65–41.7 | 4 | 18.6 |
| 40 | 50.1 | 44.7–42.7 | 4 | 22.3 | 40 | 57.5 | 44.7–42.7 | 8.5 | 21.4 | 40 | 54.95 | 44.7–43.65 | 7 | 22.4 |
| 50 | 49 | 44.7–42.7 | 11.5 | 35.48 | 50 | 58.9 | 45.7–42.7 | 19.5 | 34.2 | 50 | 58.9 | 45.7–43.65 | 10 | 33.1 |

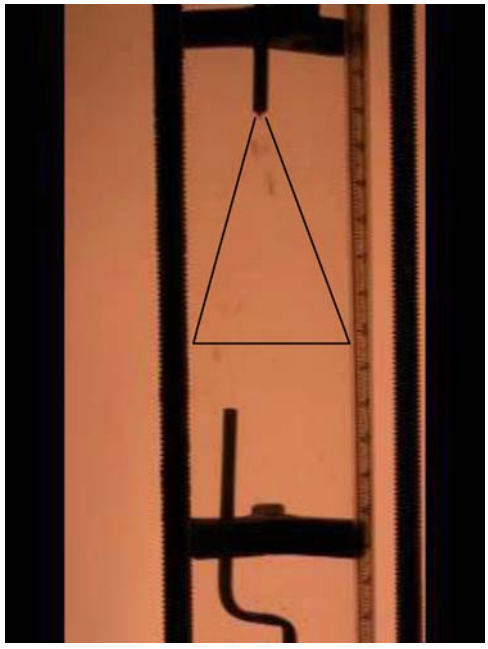

Fig. 10. Spread of the jet at Re = 8,000, 30 ppm NaOH.

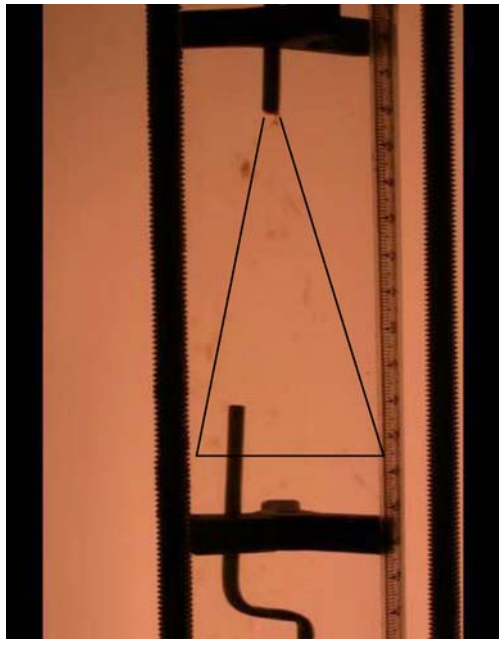

Fig. 11. Spread of the jet at Re = 8,000, 40 ppm NaOH.

brucite declined continuously, and a fourth zone in which the SI reached a terminal asymptotic value. Table 8 summarizes the data on the extent of the intermediate zone and the terminal SI of brucite.

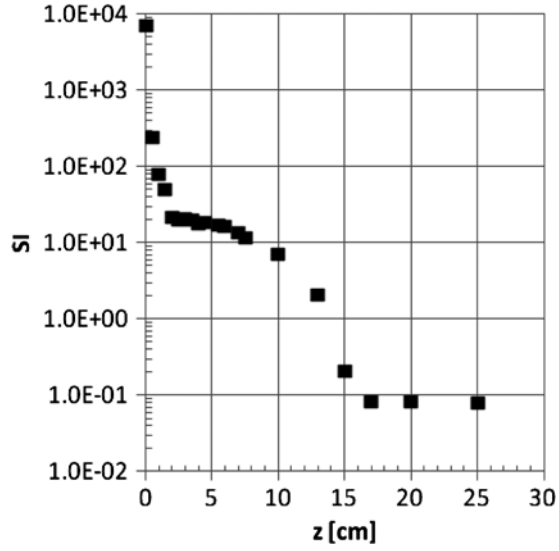


Fig. 12. SI of brucite as a function of axial distance (Re = 8,000, 30 ppm NaOH).

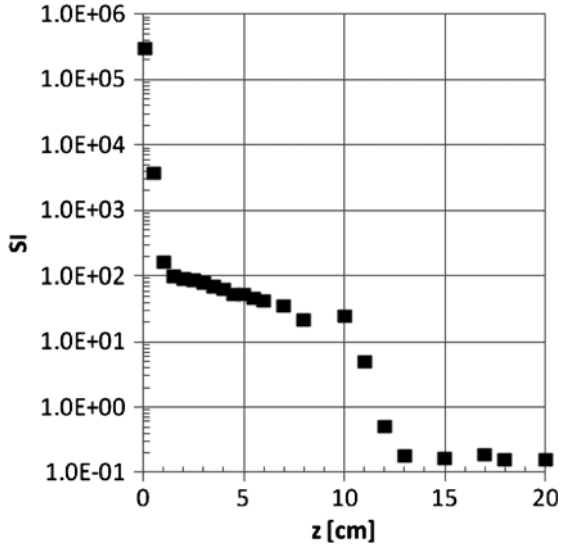


Fig. 13. SI of brucite as a function of axial distance (Re = 8,000, 40 ppm NaOH).

## 4. Correlation of the data

### *4.1. Correlation of the turbidity data*

The generalized correlations proposed by Singh and Toor (Eqs. (1) and (2)) were found to provide a rough fit to the turbidity data measured in this study. The fit could be significantly improved by the following modifications:

Table 8
Effects of the NaOH dosage and Reynolds number on the SI of brucite dissipation

| Re = 4,000 | | | | | Re = 8,000 | | | | | Re = 9,600 | | | | |
|---|---|---|---|---|---|---|---|---|---|---|---|---|---|---|
| NaOH dosage (ppm) | Initial SI level | Interm. SI level | Length interm. zone (cm) | Final SI level | NaOH dosage (ppm) | Initial SI level | Interm. SI level | Length interm. zone (cm) | Final SI level | NaOH dosage (ppm) | Initial SI level | Interm. SI level | Length interm. zone (cm) | Final SI level |
| 20 | 346 | – | – | 0.02 | 20 | 4,074 | 30.9–19.5 | 3 | 0.02 | 20 | 12,589 | 31.2–15.5 | 4 | 0.02 |
| 30 | 132 | 15.5–10.7 | 2.5 | 0.05 | 30 | 6,918 | 21.4–11.75 | 5.5 | 0.08 | 30 | 208,930 | 19.5–16.2 | 4 | 0.09 |
| 40 | 14,454 | 56.2–24.55 | 4 | 0.15 | 40 | 301,995 | 89.27–53.7 | 8.5 | 0.16 | 40 | 112,202 | 77.2–35.5 | 7 | 0.18 |
| 50 | 7,943 | 77.6–35.5 | 11.5 | 2.04 | 50 | 398,107 | 151.35–74.1 | 19.5 | 1.95 | 50 | 1,621,810 | 131.8–70.8 | 10 | 1.36 |

Entrance region correlation:

$$d^2 = 1.28\mathrm{Re}_j^{0.22} \cdot \exp\left(-0.84\frac{Z^{0.86}}{\mathrm{Re}_j^{0.5}}\right) \tag{7}$$

Fully developed region:

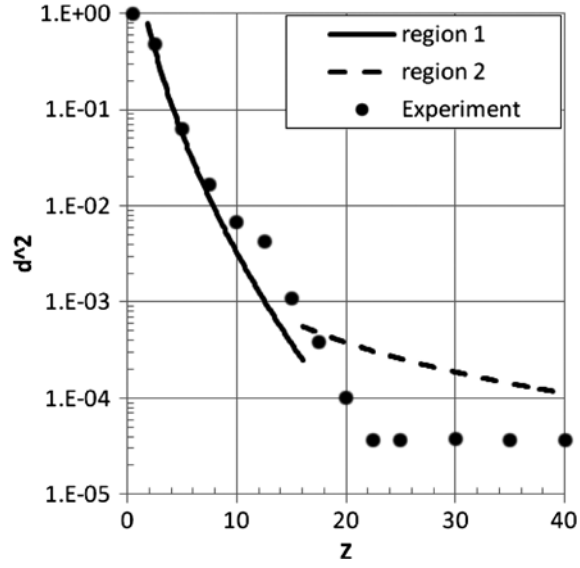


Fig. 14. Fit of turbidity data to Singh and Toor correlation (Re = 9,600, 30 ppm NaOH).

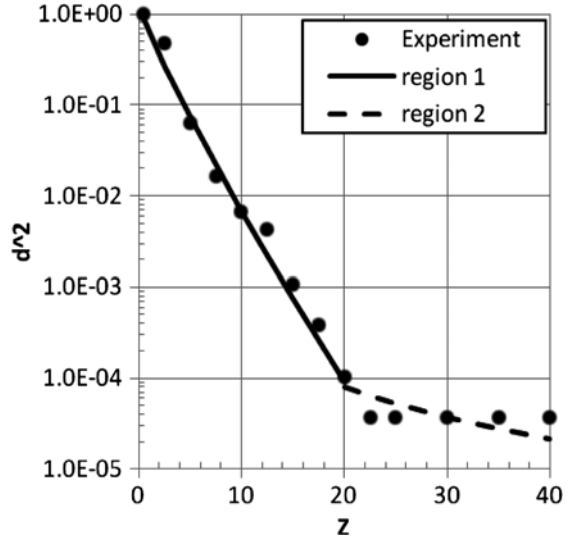


Fig. 15. Fit of turbidity data to the modified correlation (Re = 9,600, 30 ppm NaOH).

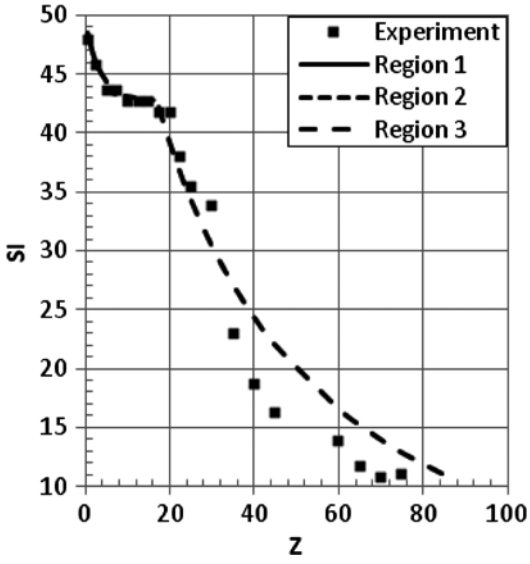


Fig. 16. Fit of the calcite SI correlation to experimental data (Re = 8,000, 20 ppm NaOH).

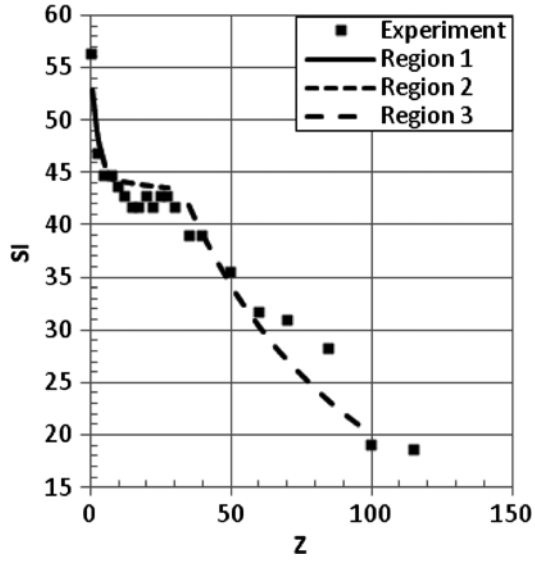


Fig. 17. Fit of the calcite SI correlation to experimental data (Re = 9,600, 30 ppm NaOH).

$$d^2 = 0.012 \cdot \frac{\mathrm{Re}_j^{2.35}}{Z^{1.35}} \tag{11}$$

Figs. 14 and 15 compare the fits provided by the Singh and Toor correlation with the fit obtained with the modified correlation for the runs carried out with a 20 ppm NaOH dosage at the Reynolds number of 9,600. A similar result was obtained in all the runs [3].

### 4.2. Correlation of the calcite SI data

The calcite SI data characterizing the three regions described in Section 3.3 were correlated by the following equations:

Initial region:

$$\mathrm{SI} = 49.16\mathrm{Re}_j^{0.22} \cdot \exp - \left(0.075\mathrm{Re}_j^{0.8} \cdot Z^{0.35}\right) \tag{9}$$

Intermediate region:

$$\mathrm{SI} = 45.7\mathrm{Re}_j^{0.036} \cdot \exp - \left(0.043\frac{Z^{0.21}}{\mathrm{Re}_j^{0.1}}\right) \tag{10}$$

Fully developed region:

$$\mathrm{SI} = \frac{101.2}{\mathrm{Re}_j^{0.028}} \cdot \exp - \left(0.19\frac{Z^{0.59}}{\mathrm{Re}_j^{0.72}}\right) \tag{11}$$

Figs. 16 and 17 compare the experimental SI data with the values calculated from the above correlations for the two runs: Re = 8,000, 20 ppm NaOH and Re = 9,600, 30 ppm NaOH. The fit in the first two regions is adequate, but is marginal in the third region.

## 5. Conclusions

The present work is a pioneering study of the precipitation phenomena which are involved in the process of injecting a concentrated NaOH solution into a desalination feed stream. The data obtained can assist in characterization of the turbidity and precipitation potential created in the injection of a concentrated NaOH solution to seawater at various Reynolds numbers and NaOH concentrations.

## References

[1] M. Singh, H.L. Toor, Characteristics of jet mixer-effect of number of jets and Reynolds numbers, AIChE J. 20 (1974) 1224–1226.
[2] C.M. Bethke, S. Yeakel, The Geochemist's Workbench (GWB) Essentials Guide– Release 8 0, 2008.
[3] V. Kesler, Injection of a concentrated solution into a flowing stream, M. Sc. thesis, Technion-Israel Institute of Technology, 2011.